arXiv:hep-ph/0411356v1 27 Nov 2004

Thermal Phase Transitions and Gapless Quark Spectra in Quark Matter at High Density

K. Iida,[1,2] T. Matsuura,[3] M. Tachibana,[2] and T. Hatsuda[3]
[1] *RIKEN BNL Research Center, Brookhaven National Laboratory, Upton, NY 11973*
[2] *The Institute of Physical and Chemical Research (RIKEN), Wako, Saitama 351-0198, Japan*
[3] *Department of Physics, University of Tokyo, Tokyo 113-0033, Japan*

Thermal color superconducting phase transitions in three-flavor quark matter at high baryon density are investigated in the Ginzburg-Landau (GL) approach. We constructed the GL potential near the boundary with a normal phase by taking into account nonzero quark masses, electric charge neutrality, and color charge neutrality. We found that the density of states averaged over paired quarks plays a crucial role in determining the phases near the boundary. By performing a weak coupling calculation of the parameters characterizing the GL potential terms of second order in the pairing gap, we show that three successive second-order phase transitions take place as the temperature increases: a modified color-flavor locked phase (ud, ds, and us pairings) → a "dSC" phase (ud and ds pairings) → an isoscalar pairing phase (ud pairing) → a normal phase (no pairing). The Meissner masses of the gluons and the number of gapless quark modes are also studied analytically in each of these phases.

PACS numbers: 12.38.-t,12.38.Mh,26.60.+c

I. INTRODUCTION

Over the past few years, the properties of color superconducting quark matter and the phase structure at high baryon density, which were originally studied in earlier publications [1], have been examined intensively (see, e.g., Ref. [2] for reviews). A color superconductor predicted to occur in weak coupling is a relativistic system in which the long-range color magnetic interaction, which is screened only dynamically by Landau-damping of exchanged gluons, is responsible for the formation of the superconducting gap. The gap in weak coupling has a non-BCS form, $\Delta \propto \mu \exp(-3\pi^2/\sqrt{2}g)$ with g the strong coupling constant and μ the quark chemical potential [3]. Furthermore, the gap has a matrix structure with $(N_c \times N_f)^2$ components due to various combinations of N_c color and N_f flavor degrees of freedom.

There is a good deal of evidence, obtained from various weak coupling analyses [4, 5, 6, 7], that if all the quark masses are zero ($m_u = m_d = m_s = 0$) and hence the quark chemical potentials are equal ($\mu_u = \mu_d = \mu_s$), the quark matter is in a color-flavor locked (CFL) phase [8] at low temperature. A transition from the CFL phase to the normal phase in mean-field theory is of second order. In weak coupling, the transition temperature T_c is related to the zero temperature gap $\Delta_{T=0}$ as $T_c = 2^{1/3} \times 0.57\Delta_{T=0}$ [9], which is a BCS relation except for a factor $2^{1/3}$.

The massless situation thus described may be approximately realized at asymptotically high densities where the quark masses are negligible compared to the quark chemical potentials. However, the effect of nonzero quark masses becomes important when the chemical potentials decrease. In the presence of a quark mass difference characterized by $2m_s/(m_u+m_d) \sim 25$, β equilibrium, electric neutrality, and color neutrality combine to produce nontrivial chemical potential differences between flavors and and between colors, leading to new phases such as the gapless CFL (gCFL) phase [10] in which two out of nine quark quasiparticles are gapless.

In our recent Letter [11], we have studied what kind of phase structure appears in β equilibrated neutral quark matter near the super-normal phase boundary when there are quark mass differences. An advantage of studying the region near the phase boundary is that in classifying the possible phase structures we can make use of the model-independent Ginzburg-Landau (GL) analysis [6, 12] in which the thermodynamic potential difference between the superfluid and normal phases is expanded in terms of the order parameter (the pairing gap). Furthermore, by calculating the parameters controlling the thermodynamic potential terms in weak coupling, one can prove which phase is realized below the super-normal boundary in the high density regime where the weak coupling analysis is valid.

A crucial observation found in Ref. [11] is that the phase structure near the critical temperature is essentially dictated by the average density of states of different quarks. We also found that the quark mass difference and the electric charge neutrality (but not the color neutrality) play key roles in determining the phase structure near the critical temperature. In weak coupling, it was shown that the following successive phase transitions occur near the super-normal phase boundary: a modified color-flavor locked (mCFL) phase (ud, ds, and us pairings) → a "dSC" phase (ud and ds pairings) → an isoscalar two-flavor superconducting (2SC) phase (ud pairing) → a normal phase (no pairing).

The purposes of this paper are (i) to give a detailed account of the results given in Ref. [11] and (ii) to investigate the elementary excitation modes (gluons with the Meissner mass, massless gluons, gapped quarks, and gapless quarks).

The content of this paper is as follows. In Sec. II, we start with a toy model that captures the essential features of the hierarchical structure of the phase transitions. Then we construct a general form of the GL potential with the quark masses in such a way that it fulfills symmetry constraints. In Sec. III, we evaluate the parameters characterizing the GL potential terms in the weak coupling region with unequal quark masses (m_i, $i{=}u,d,s$) and unequal quark chemical potentials (μ_i, $i{=}u,d,s$) by utilizing the Cornwall-Jackiw-Tomboulis (CJT) effective action [13]. In Sec. IV, we consider a simplified situation ($m_{u,d} = 0$ and $m_s \neq 0$) and calculate the corrections to the GL potential from nonzero m_s. In Sec. V, we introduce a parametrization of the gap and analyze possible phases near the super-normal phase boundary at finite temperature. For these phases, residual symmetries, the Meissner masses of gluons, and the gapped and gapless quark modes are also investigated. Section VI is devoted to summary and concluding remarks.

II. GINZBURG-LANDAU POTENTIAL

In this section, as an introduction to later sections, we first study a toy model that captures the essential features of such a hierarchical structure of phase transitions as encountered in dense quark matter. Validity of the various approximations adopted later will be also clarified by the analysis of the toy model. We then construct a general form of the GL potential with the quark masses such that it satisfies symmetry constraints.

A. A toy model

Let us assume two real order parameters, X and Y, and consider a GL potential of the following form:

$$\begin{aligned}\Omega &= \alpha(X^2+Y^2)+\delta(X^2-Y^2)\\ &\quad +\beta_1(X^2+Y^2)^2+\beta_2(X^4+Y^4).\end{aligned} \tag{1}$$

This is the most general form of the potential up to the quartic order with the "parity" symmetry, $X \leftrightarrow -X$ and $Y \leftrightarrow -Y$. For the stability of the potential, $\beta_1+\beta_2>0$ and $2\beta_1+\beta_2>0$ are implicitly assumed.

As we will see later, the coefficient α corresponds to the reduced temperature in the chiral limit, while δ denotes the degree of flavor symmetry breaking (in the present context, the breaking of $X^2 \leftrightarrow Y^2$ symmetry) which is proportional to the quark mass squared. The coefficients β_1 and β_2 are the quartic couplings that do not change sign around the critical point, but more or less receive corrections from the quark mass. Bearing in mind the results that will be obtained in later sections, we parametrize these coefficients as

$$\alpha = \mu^2 t = \mu^2\frac{T-T_c}{T_c}, \tag{2}$$

$$\delta = \mu^2\sigma = \mu^2\frac{m^2}{g\mu^2}, \tag{3}$$

$$\beta_1=\beta_2 \equiv \beta = \frac{\mu^2}{T_c^2}, \tag{4}$$

where μ and T_c are the quark chemical potential and the critical temperature in the chiral limit. m and g are the quark mass and the QCD coupling constant, respectively. In the last equalities of Eqs. (2)–(4), we mimic the actual parametric forms of t, σ, and β shown in Eqs. (28) and (61) except for numerical factors. We do not have to consider the quark mass corrections to β_1 and β_2 under the condition to be shown shortly. δ is a key parameter which governs the multiple structure of the phase transitions: Due to the presence of δ, the temperatures where the coefficients affixed to X^2 and Y^2 change sign are no longer identical.

The minimum of the potential can be simply obtained from $\partial\Omega/\partial X = \partial\Omega/\partial Y = 0$. Then one finds three different phases:

1. a phase where both X and Y have non-vanishing condensates,

$$X^2 = -\frac{1}{6\beta}(\alpha+3\delta) = -\frac{T_c^2}{6}(t+3\sigma), \tag{5}$$

$$Y^2 = -\frac{1}{6\beta}(\alpha-3\delta) = -\frac{T_c^2}{6}(t-3\sigma). \tag{6}$$

2. a phase where only Y has non-vanishing condensate,

$$X^2 = 0, \tag{7}$$

$$Y^2 = -\frac{1}{4\beta}(\alpha-\delta) = -\frac{T_c^2}{4}(t-\sigma). \tag{8}$$

3. a phase where there are no condensates,

$$X^2 = Y^2 = 0. \tag{9}$$

The behavior of the condensates as a function of the reduced temperature t is illustrated in Fig. 1. The multiple structure of the phase transitions induced by σ shown in this figure is a general feature which survives in a realistic situation that will be discussed in later sections.

The questions to be addressed here are (i) what is the region of temperature where the GL potential Eq. (1) expanded up to the quartic order is valid, and (ii) what is the justification of neglecting the quark mass corrections to β_1 and β_2. These questions can be answered if we restrict ourselves to the region

$$|t| < \mathrm{const}\cdot\sigma. \tag{10}$$

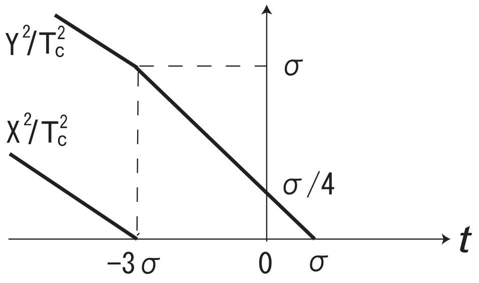

FIG. 1: Condensates X^2 and Y^2 as a function of the reduced temperature t in a toy model. σ is the parameter that breaks "flavor" symmetry $X^2 \to Y^2$.

Within this interval, both X^2 and Y^2 are of order or even smaller than σT_c^2. Therefore, the dimensionless expansion parameters of the GL potential satisfy

$$\frac{(X^2, Y^2)}{T_c^2} < \mathcal{O}(\sigma), \tag{11}$$

which in turn guarantees that the higher order terms beyond the quartic order are negligible. Furthermore, the additional quark mass corrections to β_1 and β_2 give only higher order corrections to X^2 and Y^2 as can be seen from, e.g., Eqs. (5) and (6); X^2 and Y^2 are already proportional to σ if Eq. (10) is satisfied.

B. General form of GL potential

In this subsection, we construct a general form of the GL potential on the basis of the QCD symmetry under $G = SU(3)_C \times SU(3)_L \times SU(3)_R \times U(1)_B$.

For this purpose, let us first consider a basic variable, the gap function ϕ_{bcjk}. It is defined through the pairing gap Δ for a quark (color b and flavor j) and another quark (color c and flavor k) on the Fermi surface as will be shown in Sec. III [in particular, see Eqs. (18) and (30)]. Focusing our attention on spin-zero pairings of positive energy quarks in anti-symmetric combinations of colors and of flavors, we may rewrite ϕ_{bcjk} as [6]

$$[\phi_{bcjk}]_{L,R} = \epsilon_{abc}\epsilon_{ijk}[d_a^i]_{L,R}. \tag{12}$$

Here the 3× 3 matrix $[d_a^i]_L$ belongs to the fundamental representation of $SU(3)_C \times SU(3)_L$. Similar properties hold for $[d_a^i]_R$ under the change $R \leftrightarrow L$. In this subsection, we omit the color and flavor indices and write the gap function as $\mathrm{d}_{L,R}$ for simplicity.

Under the operation of $G_{L,R} = SU(3)_C \times SU(3)_{L,R} \times U(1)_B$, the left- and right-handed quarks and the gap $\mathrm{d}_{L,R}$ transform as

$$\begin{aligned} \psi_{L,R} &\to e^{i\varphi} U_C U_{L,R} \psi_{L,R}, && (13)\\ \mathrm{d}_{L,R} &\to e^{-2i\varphi} U_{L,R} \mathrm{d}_{L,R} U_C^{\mathrm{T}}, && (14) \end{aligned}$$

where $U_{L,R}$'s are 3×3 unitary matrices corresponding to each $SU(3)_{L,R}$ symmetry. The phase factor is associated with the $U(1)_B$ rotation.

We now try to incorporate small but nonzero quark masses and write down possible terms of the GL potential allowed by the QCD symmetry G. In QCD with quark masses, we have such a term as

$$\mathcal{L} = \bar{\psi}_L m \psi_R + h.c., \tag{15}$$

with m being a 3×3 mass matrix in flavor space. Just like the standard procedure to construct the chiral Lagrangians, m is assumed to transform in the following way [14],

$$m \to U_L m U_R^\dagger. \tag{16}$$

Following the transformation laws, Eqs. (14) and (16), we can write down a possible form of the GL potential as an expansion in terms of the order parameter, which is, in the present context, the on-shell gap function $\mathrm{d}_{L,R}$. Following the discussion in Sec. II.A, we take into account the quark mass terms up to $\mathcal{O}(m^2)$ only in the quadratic terms in $\mathrm{d}_{L,R}$ and obtain

$$\begin{aligned} \Omega = {} & (a_0)_L \mathrm{Tr}(\mathrm{d}_L^\dagger \mathrm{d}_L) + (a_0)_R \mathrm{Tr}(\mathrm{d}_R^\dagger \mathrm{d}_R) \\ & + a_1[\mathrm{Tr}(\mathrm{d}_L^\dagger m \mathrm{d}_R) + h.c.] \\ & + (a_2)_L \mathrm{Tr}(\mathrm{d}_L^\dagger m m^\dagger \mathrm{d}_L) + (a_2)_R \mathrm{Tr}(\mathrm{d}_R^\dagger m^\dagger m \mathrm{d}_R) \\ & + (\hat{a}_2)_L \mathrm{Tr}(\mathrm{d}_L^\dagger \mathrm{d}_L)\mathrm{Tr}(m^\dagger m) + (\hat{a}_2)_R \mathrm{Tr}(\mathrm{d}_R^\dagger \mathrm{d}_R)\mathrm{Tr}(m^\dagger m) \\ & + c[\det m \cdot \mathrm{Tr}(\mathrm{d}_R^\dagger m^{-1} \mathrm{d}_L) + h.c.] \\ & + (b_1)_L[\mathrm{Tr}(\mathrm{d}_L^\dagger \mathrm{d}_L)]^2 + (b_1)_R[\mathrm{Tr}(\mathrm{d}_R^\dagger \mathrm{d}_R)]^2 \\ & + (b_2)_L \mathrm{Tr}[(\mathrm{d}_L^\dagger \mathrm{d}_L)^2] + (b_2)_R \mathrm{Tr}[(\mathrm{d}_R^\dagger \mathrm{d}_R)^2] \\ & + b_3 \mathrm{Tr}[(\mathrm{d}_L^\dagger \mathrm{d}_L)(\mathrm{d}_R^\dagger \mathrm{d}_R)] + b_4 \mathrm{Tr}(\mathrm{d}_L^\dagger \mathrm{d}_L)\mathrm{Tr}(\mathrm{d}_R^\dagger \mathrm{d}_R), \end{aligned} \tag{17}$$

where the a's, b's, and c are the expansion coefficients being functions of temperature and chemical potential.

Only the term proportional to a_1 in Eq. (17) breaks $U(1)_A$ symmetry and thus originates from anomaly induced interactions. It does not affect the phase structure near the super-normal phase boundary at asymptotically high density as will be shown in Sec. IV.D. The term proportional to c also does not play an important role near the phase boundary as will be discussed at the end of Sec. III.B.

We can further take into account the effects of electric and color neutralities and discuss possible terms to be included in Eq. (17). In particular, the electric charge neutrality plays a central role in this paper. Instead of writing down its general structure, we will show its explicit form calculated in the weak coupling regime in Sec. III. The effect enters into the quadratic terms of the GL potential. As for the color neutrality, its effect is subdominant in the vicinity of the phase boundary as has been already shown in Ref. [6]; the color neutrality affects only the quartic part of the GL potential (see Sec. IV.C).

III. CORRECTIONS TO THE GL POTENTIAL IN WEAK COUPLING

In this section, we calculate corrections to the GL potential by unequal quark masses (m_i, $i{=}u, d, s$) and unequal quark chemical potentials (μ_i, $i{=}u, d, s$). To simplify the derivation, we make several ansatze for the pairing gap:

1. The pairing between quarks is assumed to be in the zero total angular momentum ($J = 0$) channel [15]. Furthermore, it is assumed to be in the LL and RR channel as in the massless case and in the positive parity channel as in the presence of $U(1)_A$ breaking [2]. Then the gap can be written as $\Delta(k) = \gamma^5\Delta^{(1)} + \gamma\cdot\hat{\mathbf{k}}\gamma^0\gamma^5\Delta^{(2)}$ [1].

2. The pairing is projected onto positive energy states. In this case, it is convenient to rewrite $\Delta(k)$ as
$$\Delta(k) = \gamma^5\phi(k_0, \mathbf{k})\Lambda^+(\mathbf{k}), \tag{18}$$
where $\Lambda^+(\mathbf{k}) = (1 + \gamma^0\gamma\cdot\hat{\mathbf{k}})/2$ is a projection operator onto the positive energy states of massless quarks.

3. The pairing is assumed to take place in the color antisymmetric and flavor antisymmetric channel. This color channel is indeed the most attractive in weak coupling [3, 16, 17], while the flavor channel is chosen in such a way as to satisfy the Pauli principle. Then, the pairing gap of a quark (color b and flavor j) and another quark (color c and flavor k) at the Fermi surface takes the form as given in Eq. (12). Furthermore, the pairing in the positive parity channel is represented by
$$\mathrm{d}_L = \mathrm{d}_R \equiv d. \tag{19}$$

4. We adopt the fact that the three-momentum dependence of the on-shell gap $\Delta(q_0 = \epsilon(\mathbf{q}), \mathbf{q})$ or, equivalently, $\phi(\mathbf{q}; T) \equiv \phi(q_0 = \epsilon(\mathbf{q}), \mathbf{q})$ can be approximately factorized as [17]
$$\phi(\mathbf{q}; T) \simeq \phi(|\mathbf{q}| = \mu; T)f(\mathbf{q}), \tag{20}$$
where
$$\begin{aligned} f(\mathbf{q}) &= \sin\bar{g}y|_{T=0}, & (21)\\ \bar{g} &= g/3\sqrt{2}\pi, & (22)\\ b &\equiv 256\pi^4(2/3g^2)^{5/2}, & (23)\\ y(\mathbf{q}) &= \ln\left[\frac{2b\mu}{||\mathbf{q}| - \mu| + E(\mathbf{q})}\right], & (24)\\ E(\mathbf{q}) &= \left[||\mathbf{q}| - \mu|^2 + |\phi(\mathbf{q}; T)|^2\right]^{1/2}. & (25) \end{aligned}$$

5. We will assume later in Sec. V that d_a^i is diagonal in color-flavor space even under the influence of nonzero quark masses and charge chemical potentials. Then we will minimize the GL potential within the subspace.

In the following, we start with a known result for massless quarks (Sec. III.A) and then proceed to describe a more general situation with unequal quark masses (m_i, $i{=}u, d, s$) and unequal quark chemical potentials (μ_i, $i{=}u, d, s$) in Sec. III.B.

A. Case with massless three flavors

For a homogeneous system composed of massless quarks ($m_{u,d,s} = 0$), quarks have a common chemical potential μ, and the GL potential near the critical temperature T_c expanded up to quartic order reads [6, 18]
$$\Omega_0 = \bar{\alpha}\sum_a |\mathbf{d}_a|^2 + \beta_1(\sum_a |\mathbf{d}_a|^2)^2 + \beta_2\sum_{ab}|\mathbf{d}_a{}^* \cdot \mathbf{d}_b|^2, \tag{26}$$
where $(\mathbf{d}_a)^i \equiv (d_a^u, d_a^d, d_a^s)$, and the inner product is taken for flavor indices. Using Eq. (19), one can relate the coefficients in Eq. (17) to those in Eq. (26) as
$$\begin{aligned} \beta_1 &= (b_1)_L + (b_1)_R + b_4,\\ \beta_2 &= (b_2)_L + (b_2)_R + b_3,\\ \bar{\alpha} &= (a_0)_L + (a_0)_R. \end{aligned} \tag{27}$$
This potential is manifestly invariant under $SU(3)_C \times SU(3)_{L+R} \times U(1)_B$ rotation. In the weak coupling approximation where the one-gluon exchange force in the normal medium is responsible for the pairing, the coefficients have been calculated as [6]
$$\beta_1 = \beta_2 = \frac{7\zeta(3)}{8(\pi T_c)^2}N(\mu) \equiv \beta,\ \bar{\alpha} = 4N(\mu)t \equiv \alpha_0 t. \tag{28}$$
Here $N(\mu) = \mu^2/2\pi^2$ is the density of states at the Fermi surface, and $t = (T - T_c)/T_c$ is the reduced temperature. With the parameters in Eq. (28), one finds a single second-order phase transition at $T = T_c$ from the CFL phase ($d_a^i \propto \delta_a^i$) to the normal phase ($d_a^i = 0$) in the mean-field theory [6].

B. Case with unequal quark masses and chemical potentials

For a homogeneous system composed of unequal quark masses, there arise differences in the chemical potential among flavors and among colors due to charge and color neutrality conditions. The GL potential in this case is obtained in a similar approach to that adopted in Ref. [6] where a correction to Eq. (26) from color neutrality is calculated.

First we start with the Nambu-Gor'kov two component field ($\psi_{ai}, \bar{\psi}_{ai}^C$), where $\psi^C = C\bar{\psi}^{\mathrm{T}}$ is the charge-conjugate spinor. The quark propagator of this field with the Hartree-Fock contributions ignored in the diagonal part reads

$$G(k) \equiv \begin{pmatrix} G^{(11)}(k) & G^{(12)}(k) \\ G^{(21)}(k) & G^{(22)}(k) \end{pmatrix} \tag{29}$$

$$= \begin{pmatrix} \gamma k + \gamma^0 \mathcal{M} - m & \tilde{\Delta}(k) \\ \Delta(k) & \gamma k - \gamma^0 \mathcal{M}^{\mathrm{T}} - m \end{pmatrix}^{-1} \tag{30}$$

Here $\tilde{\Delta} = \gamma^0 \Delta^\dagger \gamma^0$, and

$$\mathcal{M}_{abij} = \delta_{ab}\delta_{ij}\mu_i, \quad m_{abij} = \delta_{ab}\delta_{ij} m_i, \tag{31}$$

are the quark chemical potentials and the quark masses in color (a, b) and flavor (i, j) space, respectively. As in Sec. III.A, we again define μ as a quark chemical potential in the chiral limit ($m_{u,d,s} = 0$). Once unequal quark masses are included under charge neutrality and β equilibrium, μ_i differs from μ. We define the deviation of $\mathcal{M}_{abij}$ from the massless case as $\delta\mathcal{M}_{abij} \equiv \delta_{ab}\delta_{ij}(\mu_i - \mu)$.

The free quark propagator G_0 and the self-energy Σ are defined from the diagonal and off-diagonal components of G^{-1} as usual:

$$G^{-1}(k) = G_0^{-1}(k) - \Sigma(k) \ . \tag{32}$$

Then the GL potential, which is a difference between the superfluid and normal phases near the critical temperature, is written in the CJT form [13]

$$\Omega = \Omega_1 + \Omega_2 \tag{33}$$

$$\Omega_1 = \frac{T}{2}\sum_n \int \frac{d^3q}{(2\pi)^3} \mathrm{Tr}[-G(q)\Sigma(q) + \ln G_0^{-1}(q)G(q)], \tag{34}$$

$$\begin{aligned} \Omega_2 = {}& g^2 \frac{T^2}{4} \sum_{m,n} \int \frac{d^3k}{(2\pi)^3} \int \frac{d^3q}{(2\pi)^3} \\ & \times \mathrm{Tr}\Big[\mathcal{D}^{\alpha\beta}_{\mu\nu}(q-k)\gamma^\mu \frac{\lambda^\alpha}{2} G^{(12)}(k)\gamma^\nu \left(\frac{\lambda^\beta}{2}\right)^{\mathrm{T}} G^{(21)}(q) \\ & + \mathcal{D}^{\alpha\beta}_{\mu\nu}(q-k)\gamma^\mu \left(\frac{\lambda^\alpha}{2}\right)^{\mathrm{T}} G^{(21)}(k)\gamma^\nu \frac{\lambda^\beta}{2} G^{(12)}(q)\Big]. \end{aligned} \tag{35}$$

Here Ω_2 represents the two particle irreducible graphs in the mean-field approximation with $\mathcal{D}(q)$ being the gluon propagator in hard dense loop approximation, and λ^α the generators of color $SU(3)$. The summations are taken over Matsubara frequencies of quarks.

In the following, we will consider the corrections from $\delta\mathcal{M}_{abij}$ and m_{abij} to the quadratic term in Δ assuming that the corrections are small. The corrections to the quartic terms are negligible near the critical temperature. Figure 2 represents the $\mathcal{O}(\Delta^2)$ contributions to Ω_1 and Ω_2.

First we consider $\Omega_1^{\Delta^2}$,

$$\begin{aligned} \Omega_1^{\Delta^2} &= -\frac{T}{2}\sum_{n \text{ odd}} \int \frac{d^3q}{(2\pi)^3} \mathrm{Tr}\left[\frac{1}{\gamma q + \gamma^0 \mathcal{M} - m}\tilde{\Delta}(q) \right. \\ & \qquad \left. \times \frac{1}{\gamma q - \gamma^0 \mathcal{M}^{\mathrm{T}} - m}\Delta(q)\right] \\ &= -\sum_{abij} \frac{i}{4} \oint \frac{d^4q}{(2\pi)^4} \tanh\left(\frac{q_0}{2T}\right) \mathrm{Tr}\left[\frac{1}{\gamma q + \gamma^0\mu_i - m_i} \right. \\ & \qquad \left. \times \tilde{\Delta}(q)_{abij} \frac{1}{\gamma q - \gamma^0 \mu_j - m_j}\Delta(q)_{baji}\right]. \end{aligned} \tag{36}$$

The first quark propagator in the right-hand side of Eq. (36) has particle and anti-particle poles,

$$\epsilon^{p\pm} = \pm|\mathbf{q}| - p_F^i, \tag{37}$$

while the second propagator has hole and anti-hole poles,

$$\epsilon^{h\mp} = \mp|\mathbf{q}| + p_F^j, \tag{38}$$

where $p_F^i = \sqrt{\mu_i^2 - m_i^2}$ is the Fermi momentum of flavor i. We define the shift of the chemical potential of flavor i from μ as

$$\delta\mu_i = \mu_i - \mu. \tag{39}$$

Then, up to $\mathcal{O}(m^2/\mu^2, \delta\mu/\mu)$, p_F^i can be written as

$$p_F^i \simeq \mu_i - m_i^2/2\mu. \tag{40}$$

Of the poles in Eqs. (37) and (38), only two of them, $q_0 = \epsilon^{p+}$ (particles) and $q_0 = \epsilon^{h-}$ (particle holes), have relevant contributions to the potential. The other two poles contribute to the gaps on antiparticle (antiparticle hole) mass shell, which are irrelevant in our calculation. Let us define

$$\tilde{q} = |\mathbf{q}| - \mu, \tag{41}$$

$$\mathcal{F}(\tilde{q}) = \frac{\tanh(\tilde{q}/2T)}{\tilde{q}}. \tag{42}$$

Then, combining the residues of the two poles, we obtain

$$\Omega_1^{\Delta^2} = \sum_{abij} \frac{1}{2} \int \frac{d^3q}{(2\pi)^3} \left(\mathcal{F}(\tilde{q}) - \frac{\partial \mathcal{F}(\tilde{q})}{\partial \tilde{q}}\delta p_{ij}\right) |\phi_{abij}|^2. \tag{43}$$

Here,

$$\delta p_{ij} = (p_F^i + p_F^j)/2 - \mu. \tag{44}$$

For later purpose, we also introduce an averaged shift of the chemical potential as

$$\delta\mu_{ij} = (\delta\mu_i + \delta\mu_j)/2. \tag{45}$$

In the diagrammatic language, the first term in the right-hand side of Eq. (43) corresponds to (a0) in Fig.

2. The second term corresponds to (a1) and (a2). (a3) vanishes because of the Lorentz structure of the gaps together with the identity, $\mathrm{Tr}(\Lambda^+\Lambda^-) = 0$.

To perform the momentum integration in Eq. (43), it is convenient to introduce a positive constant $\kappa \sim \mathcal{O}(g^{-1})$ which cancels at the end of the calculation [6, 17]. The cutoff of the three-momentum Λ is taken to be $b\mu$ for the sake of consistency with the formula, Eq. (21). We divide the region of the momentum integral $-\mu < |\mathbf{q}| - \mu < b\mu$ into two parts, $0 < ||\mathbf{q}| - \mu| < \kappa\phi_0$ (region I), and $-\mu < |\mathbf{q}| - \mu < -\kappa\phi_0$ and $\kappa\phi_0 < |\mathbf{q}| - \mu < b\mu$ (region II) [17]. Here we defined $\phi_0 \equiv [(1/9)\sum_{abij} |\phi_{abij}(\mu, T = 0)|^2]^{1/2}$. In each region, the following approximations can be safely taken: in region I, $\sin \bar{g}y|_{T=0} \sim 1$, and in region II, $\tanh[(|\mathbf{q}| - \mu)/2T] \sim (|\mathbf{q}| - \mu)/||\mathbf{q}| - \mu|$.

The first term in the right-hand side of Eq. (43) is calculated as

$$\begin{aligned}
(\mathrm{a0}) &= \sum_{abij} \frac{1}{2} \int \frac{d^3q}{(2\pi)^3}\, \mathcal{F}(\tilde{q})\, |\phi_{abij}|^2 \\
&= \sum_{abij} \frac{1}{2} N(\mu) \Bigg\{ 2 \int_0^{\kappa\phi_0} d\tilde{q}\, \mathcal{F}(\tilde{q}) \\
&- \left(\int_{\ln(b\mu/\kappa\phi_0)}^{\ln b} + \int_{\ln(b\mu/\kappa\phi_0)}^{0} \right) dy f^2(y) \Bigg\} |\phi_{abij}|^2 \\
&= \sum_{abij} N(\mu) \left\{ \ln\left(\frac{T_c}{T}\right) + \frac{\pi}{4\bar{g}} \right\} |\phi_{abij}|^2. \qquad (46)
\end{aligned}$$

In the first equality, we replaced the momentum in the measure by the density of states at the Fermi surface. In the second equality, we used the weak coupling approximation $g \ll 1$ and expanded $f(y)$ in terms of g. We also used the explicit g dependence of T_c and ϕ_0 in weak coupling [16, 17], $\ln(T_c/\mu) \sim \ln(\phi_0/\mu) \sim -3\pi^2/\sqrt{2}g$, to obtain the final form.

The second term in the right-hand side of Eq. (43) is more involved:

$$\begin{aligned}
(\mathrm{a1}) &+ (\mathrm{a2}) \\
&= -\frac{1}{2} \int \frac{d^3q}{(2\pi)^3} \frac{\partial \mathcal{F}(\tilde{q})}{\partial \tilde{q}}\, \delta p\, |\phi|^2 \\
&= \frac{1}{4\pi^2} \int_{-\mu}^{b\mu} d\tilde{q}\, (\tilde{q} + \mu)^2 \{\mathcal{F}(\tilde{q}) - \mathcal{F}(\tilde{q} + \delta p)\} f^2(\tilde{q})\, |\phi|^2 \\
&\sim \frac{1}{4\pi^2} \Bigg[\left\{ \int_{-\mu}^{b\mu} - \int_{-\mu+\delta p}^{b\mu+\delta p} \right\} d\tilde{q}\, \mathcal{F}(\tilde{q}) f^2(\tilde{q}) (\tilde{q} + \mu)^2 \\
&\qquad + 2\, \delta p \int_{-\mu}^{b\mu} d\tilde{q}\, \mathcal{F}(\tilde{q}) f^2(\tilde{q}) (\tilde{q} + \mu) \Bigg] |\phi|^2 \\
&\sim \frac{1}{4\pi^2} \Bigg[-\mathcal{F}(b\mu) f^2(b\mu)(b\mu + \mu)^2 \\
&\qquad + 2 \int_{-\mu}^{b\mu} d\tilde{q}\, \mathcal{F}(\tilde{q}) f^2(\tilde{q}) (\tilde{q} + \mu) \Bigg] \delta p\, |\phi|^2, \qquad (47)
\end{aligned}$$

where we abbreviated internal indices for simplicity. $f(b\mu)$ appearing in the first term of the last bracket in Eq. (47) is $\mathcal{O}(g(\phi^2/(b\mu)^2))$ and can be neglected at high densities. Then the second term leads to

$$\begin{aligned}
(\mathrm{a1}) &+ (\mathrm{a2}) \\
&= \frac{1}{2\pi^2} \mu\, \delta p \Bigg\{ 2 \int_0^{\kappa\phi_0} d\tilde{q}\, \mathcal{F}(\tilde{q}) \\
&- \left(\int_{\ln(b\mu/\kappa\phi_0)}^{\ln b} + \int_{\ln(b\mu/\kappa\phi_0)}^{0} \right) dy f^2(y) \Bigg\} |\phi|^2 \\
&= -N(\mu) \frac{\delta p}{\mu} \ln\left(\frac{T_c}{\mu}\right) |\phi|^2. \qquad (48)
\end{aligned}$$

Here we again expanded $f(y)$ in terms of g and used the explicit g dependence of T_c in weak coupling to obtain the final form.

Then the sum of Eqs. (46) and (48) becomes

$$\begin{aligned}
\Omega_1^{\Delta^2} &= (\mathrm{a0}) + (\mathrm{a1}) + (\mathrm{a2}) \\
&= \sum_{abij} N(\mu) \Bigg[\left\{ \ln\left(\frac{T_c}{T}\right) + \frac{\pi}{4\bar{g}} \right\} \\
&- \frac{\delta p_{ij}}{\mu} \ln\left(\frac{T_c}{\mu}\right) \Bigg] |\phi_{abij}|^2. \qquad (49)
\end{aligned}$$

Let us next evaluate $\Omega_2^{\Delta^2}$. In the diagrammatic description, this corresponds to (b0)–(b4) in Fig. 2 in which the quark propagator is expanded in powers of masses and chemical potential differences. Of these graphs, (b2) vanishes because of the Lorentz structure of the gaps, and (b3) vanishes because the gaps are constructed by quarks having the same chirality. As a result, only (b0),

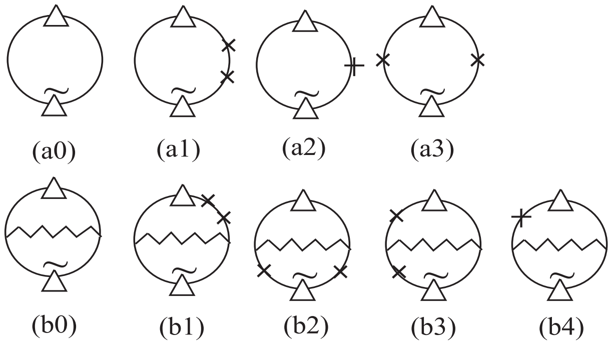

FIG. 2: The quadratic terms of the GL potential. × and + represent m and $\delta\mu$, respectively. (a0)–(a3) represent $\Omega_1^{\Delta^2}$, and (b0)–(b4) are the two particle irreducible graphs $\Omega_2^{\Delta^2}$. (a0) and (b0) are the quadratic terms of the potential in the $m = \delta\mu = 0$ case. Among these graphs, (a3) and (b2) vanish due to the Lorentz structure of the gap. (b3) vanishes because we consider the gaps constructed by quarks having the same chirality. Only (a1), (a2), (b1), and (b4) give finite correction to the original GL potential [(a0) plus (b0)].

(b1), and (b4) have a finite value. We expand these diagrams by $t \equiv |T - T_c|/T_c$ around T_c up to $\mathcal{O}(t)$ for (b0) and $\mathcal{O}(1)$ for (b1) and (b4).

We use a relation between T_c and g when m_i and $\delta\mu_i$ in the denominator of the quark propagator are taken to be zero [6],

$$f(\mathbf{q}) = -g^2 \frac{1}{2} \oint \frac{d^4k}{(2\pi)^4} \tanh\left(\frac{k_0}{2T_c}\right) \mathrm{Tr}\Big[\mathcal{D}^{\alpha\beta}_{\mu\nu}(q-k)\gamma^\mu \times \left(\frac{\lambda^\alpha}{2}\right)^{\mathrm{T}} (\gamma k - \gamma^0 \mathcal{M})^{-1} (\gamma k + \gamma^0 \mathcal{M})^{-1} \gamma^\nu \left(\frac{\lambda^\beta}{2}\right) f(\mathbf{k})\Big]. \tag{50}$$

This equation is derived by taking $T \to T_c$ in the gap equation with the decomposition Eq. (20).

Using Eq. (50) which relates T_c and g, we can evaluate (b0), (b1), and (b4) in Fig. 2. We derive (b0) as follows. In leading order in t, (b0) becomes

$$\begin{aligned}
(\mathrm{b0}) \;\to\; & \frac{i}{4} \oint \frac{d^4q}{(2\pi)^4} \tanh\left(\frac{q_0}{2T_c}\right) \\
& \times \mathrm{Tr}\Bigg[\Bigg(-g^2 T_c \sum_{n\ \mathrm{odd}} \int \frac{d^3k}{(2\pi)^3} \mathcal{D}^{\alpha\beta}_{\mu\nu}(q-k)\gamma^\mu \left(\frac{\lambda^\alpha}{2}\right)^{\mathrm{T}} \\
& \quad \times G^{(21)}(k)\gamma^\nu \left(\frac{\lambda^\beta}{2}\right)\Bigg) G^{(12)}(q)\Bigg]\Bigg|_{T=T_c} \\
= \; & \frac{i}{4} \oint \frac{d^4q}{(2\pi)^4} \tanh\left(\frac{q_0}{2T}\right) \\
& \quad \times \mathrm{Tr}\left[f(\mathbf{q})\phi(T) G^{(12)}(q)\right]\Bigg|_{T=T_c} \\
= \; & \frac{i}{4} \oint \frac{d^4q}{(2\pi)^4} \tanh\left(\frac{q_0}{2T}\right) \mathrm{Tr}[\Delta(q) G^{(12)}(q)]\Bigg|_{T=T_c} \\
= \; & -\Omega_1^{\Delta^2}|_{T=T_c}.
\end{aligned} \tag{51}$$

The $\mathcal{O}(t)$ term of (b0) becomes

$$\begin{aligned}
& (\mathrm{b0}) \to \\
& (T-T_c)\frac{i}{4}\frac{d}{dT}\Bigg\{\oint \frac{d^4k}{(2\pi)^4} \tanh\left(\frac{k_0}{2T}\right) \mathrm{Tr}[G^{(21)}(k)\tilde{\Delta}(k)] \\
& + \oint \frac{d^4q}{(2\pi)^4} \tanh\left(\frac{q_0}{2T}\right) \mathrm{Tr}[\Delta(q) G^{(12)}(q)]\Bigg\}\Bigg|_{T=T_c} \\
& = 2(T-T_c)\frac{d}{dT}(-\Omega_1^{\Delta^2})|_{T=T_c}.
\end{aligned} \tag{52}$$

(b1) and (b4) can be calculated in a similar way, and they become

$$(\mathrm{b1}) + (\mathrm{b4}) = N(\mu) \frac{2\delta p_{ij}}{\mu} \ln\left(\frac{T_c}{\mu}\right) \; |\phi_{abij}|^2. \tag{53}$$

Adding (b1) and (b4) to (b0), we finally obtain

$$\begin{aligned}
\Omega_2^{\Delta^2} \;=\; & (\mathrm{b0}) + (\mathrm{b1}) + (\mathrm{b4}) \\
=\; & -\Omega_1^{\Delta^2}|_{T=T_c} + 2(T-T_c)\frac{d}{dT}(-\Omega_1^{\Delta^2})|_{T=T_c} \\
& \quad + N(\mu)\frac{2\delta p_{ij}}{\mu} \ln\left(\frac{T_c}{\mu}\right) \; |\phi_{abij}|^2 \\
=\; & \sum_{abij} N(\mu) \left\{-\frac{\pi}{4\bar{g}} + 2\ln\left(\frac{T}{T_c}\right) + \frac{2\delta p_{ij}}{\mu} \ln\left(\frac{T_c}{\mu}\right) \right\} \\
& \quad \times |\phi_{abij}|^2.
\end{aligned} \tag{54}$$

Combining Eqs. (49) and (54), we obtain the final result for the quadratic term of the GL free energy,

$$\Omega_{GL}^{\Delta^2} = \sum_{abij} N(\mu) \left\{ \ln\left(\frac{T}{T_c}\right) - \frac{\delta p_{ij}}{\mu} \ln\left(\frac{\mu}{T_c}\right) \right\} \times |\phi_{abij}|^2, \tag{55}$$

$$\delta p_{ij} \simeq \delta\mu_{ij} - (m_i^2 + m_j^2)/(4\mu). \tag{56}$$

It can be rewritten in a clearer form,

$$\Omega_{GL}^{\Delta^2} = \sum_{abij} N(\mu) \left(\frac{T - T_c^{ij}}{T_c}\right) |\phi_{abij}|^2, \tag{57}$$

$$\frac{T_c^{ij}}{T_c} = 1 + \frac{\delta p_{ij}}{\mu} \ln\left(\frac{\mu}{T_c}\right). \tag{58}$$

Several comments are in order here.

- The free energy correction depends only on the average shift of the Fermi momenta of paired quarks, δp_{ij}, as can be seen from Eq. (55). Furthermore, the correction may be decomposed into a sum of the effects from the averaged chemical potential and the averaged mass squared when δp_{ij} is small, as shown in Eq. (56).
- Equations (57) and (58) indicate that the shift δp_{ij} affects the free energy correction through the critical temperature T_c^{ij} for the (i, j) pairing. The larger the shift δp_{ij} is, the higher the melting temperature T_c^{ij} becomes. In other words, one can compare the thermal stability of two different pairs only by taking note of a difference in the average density of states between them.
- The unlocking at $T = 0$ is different in mechanism from our unlocking near T_c. At $T = 0$, color-flavor unlocking due to the Fermi momentum *mismatch* between paired quarks is expected at $\mu \sim m_s^2/\phi_0$ [19]. In contrast, the Fermi momentum *average* is important for our unlocking near T_c.
- We can see that in the correction obtained above quark flavors do not mix with each other. As long as we consider the pairing of positive energy quarks and neglect that of antiquarks, the flavor structure of a gap always enters in the form of m_i^2 instead of $m_i m_j (i \neq j)$.

IV. GL POTENTIAL IN REALISTIC QUARK MATTER

Up to now we constructed the GL potential for general quark masses and chemical potential shifts assuming that the corrections are small. In this section, we will focus on the case close to a realistic situation by taking $m_s \neq 0$ with $m_{u,d} = 0$ and by imposing β equilibrium and charge neutrality conditions. This analysis clarifies the role of the strange quark mass in possible phase structures near the super-normal phase boundary at finite T.

A. Direct m_s correction through the quark mass term

Let us first consider the correction directly proportional to m_s^2 in Eqs. (55) and (56). It is easy to see from the flavor structure of Eq. (55) that m_s affects only us and ds pairings. This is also reasonable from the physical point of view as will be shown below.

By inserting $m_s \neq 0$ with $m_{u,d} = 0$ and using Eq. (12) with Eq. (19), the direct m_s correction in Eq. (55) becomes

$$\epsilon \sum_a (|d_a^u|^2 + |d_a^d|^2) = \epsilon \sum_a (|\mathbf{d}_a|^2 - |d_a^s|^2). \tag{59}$$

Here the coefficient ϵ reads

$$\epsilon \simeq \alpha_0 \frac{m_s^2}{4\mu^2} \ln\left(\frac{\mu}{T_c}\right) \sim 2\alpha_0\sigma, \tag{60}$$

where $\alpha_0 = 4N(\mu)$ is defined in Eq. (28), and a dimensionless parameter σ is introduced as

$$\sigma = \left(\frac{3\pi^2}{8\sqrt{2}}\right) \frac{m_s^2}{g\mu^2}. \tag{61}$$

In Eq. (60) we have used a weak coupling relation, $\ln(T_c/\mu) \sim -3\pi^2/(\sqrt{2}g)$, which originates from the long-range color magnetic interaction [16, 17].

Since the finite m_s decreases the Fermi momentum of s quarks, δp_{us} and δp_{ds} are smaller than δp_{ud}, and thus ϵ becomes positive such that ud pairing is favored over us and ds pairings. Consequently, the CFL phase becomes asymmetric in flavor space and its critical temperature is lowered, leading to the appearance of the 2SC phase ($d_a^i \propto \delta^{is}$) just below T_c [20].

B. Indirect m_s correction through the charge chemical potentials

We proceed to discuss the correction from the charge chemical potentials, which is proportional to $\delta\mu_{ij}$ in Eqs. (55) and (56). Under β equilibrium and charge neutrality, the electron chemical potential μ_e and the shift $\delta\mu_i$ of the chemical potential of flavor i are related as

$$\delta\mu_i = -q_i\mu_e \tag{62}$$

with q_i being the electric charges of the quarks; $q_u = 2/3$ and $q_{d,s} = -1/3$. In weak coupling, where one may regard normal quark matter and electrons as noninteracting Fermi gases, μ_e is related to m_s as

$$\mu_e = m_s^2/4\mu. \tag{63}$$

This estimate is valid in the vicinity of T_c where corrections to μ_e by a finite pairing gap affect only the quartic terms in the GL potential.

By inserting Eqs. (62) and (63) and using Eq. (12) with Eq. (19), the indirect m_s correction in Eq. (55) becomes

$$\eta \left(\frac{1}{3}\sum_a |\mathbf{d}_a|^2 - \sum_a |d_a^u|^2\right). \tag{64}$$

Here the coefficient η reads

$$\eta \simeq \alpha_0 \frac{m_s^2}{8\mu^2} \ln\left(\frac{\mu}{T_c}\right) \sim \alpha_0\sigma. \tag{65}$$

Since $\delta\mu_{ds}$ is larger than $\delta\mu_{ud}$ and $\delta\mu_{us}$ and it increases the average Fermi momentum of ds quarks in Eq. (56), the indirect m_s correction favors ds pairing than ud and us pairings.

Note that we only consider the modification of T_c due to nonzero m_s through the properties of the superfluid phase. Actually, T_c is modified not only by the properties of the superfluid phase but also of the normal phase. The modification by the normal phase enters through the Debye mass in the gluon propagator $\mathcal{D}$ in the relation between T_c and g, Eq. (50). Fortunately the modification due to nonzero m_s and charge neutrality in normal quark matter is like $T_c \to T_c(1 + \mathcal{O}(g\sigma))$. This modification is of higher order than that in superfluid quark matter, $T_c \to T_c(1 + \mathcal{O}(\sigma))$, to be derived in Sec. V.

C. Effect of color neutrality

We consider color neutrality of the system as well. In contrast to the case at $T = 0$, however, it affects only the quartic terms in the GL potential because the possible chemical potential differences between colors are [6, 21]

$$\delta\mu_{ab} = -\frac{1}{9\mu} \ln\left(\frac{T_c}{\mu}\right) [3\sum_i (d_a^i d_b^{i*}) - \delta_{ab} \sum_{c,i} |d_c^i|^2], \tag{66}$$

which are already of quadratic order in the gap. Here $\delta\mu_{ab} = \mu_{ab} - \mu\delta_{ab}$, and μ_{ab} is the chemical potential conjugate to $n_{ab} = \sum_i \bar{\psi}_{bi}\gamma^0\psi_{ai}$ [6]. In weak coupling the magnitude of the correction to the quartic terms is suppressed by $\mathcal{O}((T_c/g\mu)^2)$ compared to the leading quartic terms. Thus color neutrality has no essential consequence to the phase transitions considered in this paper. A major difference between the corrections from the charge neutrality and the color neutrality is that the former shifts the quark chemical potentials even in the normal phase, while the latter works only when the pairing occurs. This is why the former is more important than the latter near T_c.

D. Effect of instantons

In QCD with three flavors, instantons induce chirality-flipping six-fermion interactions. This interaction leads to a sextic term in the gap in the chiral limit, which is irrelevant near the super-normal phase boundary. If the strange quark mass enters, the direct instantons induce an effective four-fermion interaction between u and d quarks [22]. This leads to a quadratic term in the GL potential, $\xi \sum_a |d_a^s|^2$, which corresponds to the a_1 term in Eq. (17). An explicit calculation in weak coupling shows that $\xi \sim -\alpha_0 (m_s/\mu)(\Lambda_{\rm QCD}/\mu)^9 (1/g)^{14}$. The negative sign indicates that the instanton effect favors ud pairing as does one-gluon exchange [see Eq. (59)]. However, the magnitude of ξ is highly suppressed at high densities. Therefore we will ignore this term in the following.

In summary of Secs. IV.A–D, as far as we are close to the super-normal phase boundary at high density, we have only to consider the corrections from the strange quark mass and the electric charge neutrality, which favor ud pairing and ds pairing, respectively.

E. Validity of the approximations

Our analysis of the GL potential near T_c is valid as long as (a) $g \ll 1$, (b) $\sigma \ll 1$, and (c) $T_c \ll g\mu$. The condition (a) is necessary for the dominance of the long-range magnetic interaction acting between quarks. The condition (b) allowed us to consider the corrections to the GL potential by the strange quark mass and differences in the chemical potential among flavors up to quadratic order in the gap. The condition (c) is imposed so that the correction to the quartic terms in the GL potential from the color neutrality can be neglected. These conditions are all satisfied at asymptotically high density.

If we use the result for T_c calculated in weak coupling [16, 17], one finds that (c) is a consequence of (a). The conditions (a) and (b) can also be combined into

$$\frac{m_s^2}{\mu^2} \ll g \ll 1. \tag{67}$$

V. MELTING PATTERN OF DIQUARK CONDENSATES

In this section, we clarify the phase structure near the transition temperature using the GL potential corrected by Eqs. (59) and (64). We start from assuming the form of the condensation and derive the temperature dependence of the gaps that minimize the potential. Then we discuss the properties of quark quasiparticles and transverse gluons in each of the phases near the transition temperature.

A. Phase structure with finite m_s and charge neutrality

Since the two effects of nonzero m_s, characterized by Eqs. (59) and (64), favor ud pairing and ds pairing, respectively, the finite temperature transition from the CFL to the normal phase at $m_s = 0$ is significantly modified. In fact, as we show in detail below, successive color-flavor unlockings take place instead of a simultaneous unlocking of all color-flavor combinations. To describe this *hierarchical thermal unlocking*, it is convenient to introduce a parameterization

$$d_a^i = \begin{pmatrix} \Delta_1 & 0 & 0 \\ 0 & \Delta_2 & 0 \\ 0 & 0 & \Delta_3 \end{pmatrix}. \tag{68}$$

We assume $\Delta_{1,2,3}$ to be real. We also name the phases for later convenience as [11]

$$\begin{array}{lll} \Delta_{1,2,3} \neq 0 & & : \text{mCFL}, \\ \Delta_1 = 0, & \Delta_{2,3} \neq 0 & : \text{uSC}, \\ \Delta_2 = 0, & \Delta_{1,3} \neq 0 & : \text{dSC}, \\ \Delta_3 = 0, & \Delta_{1,2} \neq 0 & : \text{sSC}, \\ \Delta_{1,2} = 0, & \Delta_3 \neq 0 & : \text{2SC}, \end{array} \tag{69}$$

where dSC (uSC, sSC) stands for superconductivity in which for d (u, s) quarks all three colors are involved in the pairing.

In terms of the parameterization (68), the GL potential with corrections of $\mathcal{O}(m_s^2)$ to the quadratic term, Eqs. (59) and (64), reads

$$\begin{aligned} \Omega &= \bar{\alpha}'(\Delta_1^2 + \Delta_2^2 + \Delta_3^2) - \epsilon\Delta_3^2 - \eta\Delta_1^2 \\ &+ \beta_1(\Delta_1^2 + \Delta_2^2 + \Delta_3^2)^2 + \beta_2(\Delta_1^4 + \Delta_2^4 + \Delta_3^4), \end{aligned} \tag{70}$$

where $\bar{\alpha}' = \bar{\alpha} + \epsilon + \dfrac{\eta}{3}$.

We proceed to analyze the phase structure dictated by Eq. (70) with the weak coupling parameters (28), (60), and (65) up to leading order in g. A stable condensation must satisfy the gap equations

$$\partial\Omega/\partial\Delta_{1,2,3} = 0, \tag{71}$$

and it must minimize the potential Eq. (70). We compare the energies of all condensates in Eq. (69) and decide the most stable condensation at each temperature near T_c.

In Figs. 3 and 4 the results thus obtained for the phase structure near T_c are summarized.

Figure 3(a) shows the second-order phase transition, CFL → normal for $m_s = 0$. Figures 3(b,c) represent how

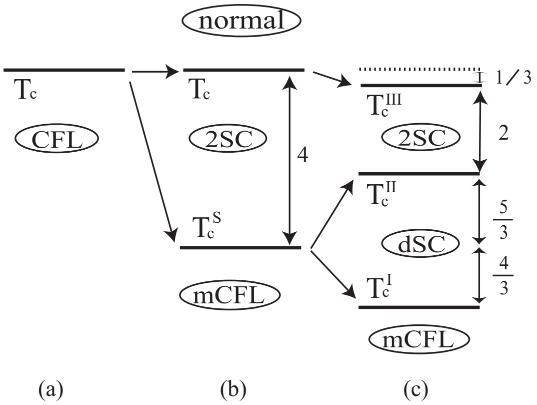

FIG. 3: Transition temperatures of the three-flavor color superconductor in weak coupling: (a) all quarks are massless; (b) nonzero m_s in the quark propagator is considered; (c) electric charge neutrality is further imposed. The numbers attached to the arrows are in units of σT_c. From Ref. [11].

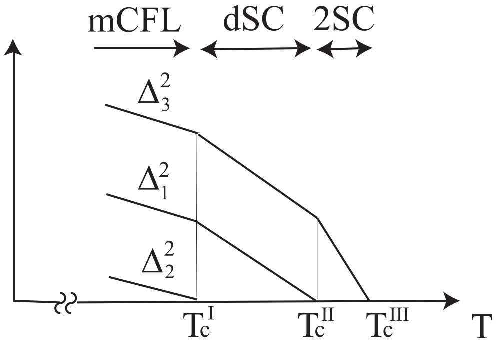

FIG. 4: A schematic illustration of the gaps squared as a function of T. From Ref. [11].

the phase transitions and their critical temperatures bifurcate as we introduce (b) effects of a nonzero m_s in the quark propagator and then (c) effects of charge neutrality. In case (b), two second-order phase transitions arise: mCFL (with $\Delta_1 = \Delta_2$) → 2SC at $T = T_c^s \equiv (1-4\sigma)T_c$, and 2SC → normal at $T = T_c$. In case (c), there arise three successive second-order phase transitions, mCFL → dSC at $T = T_c^{\rm I}$, dSC → 2SC at $T = T_c^{\rm II}$, and 2SC → normal at $T = T_c^{\rm III}$. Shown in Fig. 4 is the T-dependence of the gaps $\Delta_{1,2,3}$ for the case (c). All the gaps are continuous functions of T, but their slopes are discontinuous at the critical points, which reflects the second order nature of the transitions in the mean-field treatment of Eq. (70).

We may understand the bifurcation of the transition temperatures as follows. In the massless case (a), T_c is degenerate between the CFL and 2SC phases, the chemical potential is common to all three flavors and colors, and the CFL phase is more favorable than the 2SC phase below T_c. As one goes from (a) to (b), the density of states of the s quarks at the Fermi surface is reduced. Then the critical temperature for the CFL phase is lowered, and the 2SC phase is allowed to appear at temperatures between T_c^s and T_c. As one goes from (b) to (c), the average chemical potential of ds (ud and us) quarks increases (decreases). Accordingly, the transition temperatures further change from T_c to $T_c^{\rm III}$ and from T_c^s to $T_c^{\rm I}$ and $T_c^{\rm II}$.

Now we examine in more detail how the color-flavor unlocking in case (c) proceeds with increasing T from the region below $T_c^{\rm I}$.

(i) Just below $T_c^{\rm I}$, we have a CFL-like phase, but the three gaps take different values, with an order $\Delta_3 > \Delta_1 > \Delta_2 \neq 0$ (the mCFL phase). The reason why this order is realized can be understood from the GL potential (70). The ϵ-term and η-term in Eq. (70) tend to destabilize us pairing (Δ_2) relative to ud pairing (Δ_3) and ds pairing (Δ_1), and since $\epsilon > \eta (> 0)$, ds pairing is destabilized more effectively than ud pairing. The value of each gap in the mCFL phase reads

$$\Delta_i^2 = \frac{\alpha_0}{8\beta}\left(\frac{T_c - T}{T_c} + c_i\sigma\right), \tag{72}$$

with $c_{1,2,3} = (-4/3, -16/3, 8/3)$. The mCFL phase has only a global symmetry $U(1)_{C+L+R} \times U(1)_{C+L+R}$ in contrast to the global symmetry $SU(3)_{C+L+R}$ in the CFL phase with $m_{u,d,s} = 0$. The remaining $U(1)$ generators are

$$\begin{aligned} \mathcal{Q}_1 &= T_3 - S_3, \\ \mathcal{Q}_2 &= T_8 - S_8. \end{aligned} \tag{73}$$

Here T_a (S_i) are the part of the generators of $SU(3)_C$ ($SU(3)_{L+R}$) with explicit forms $T_3 = S_3 = (1/2)\mathrm{diag}(1,-1,0)$ and $T_8 = S_8 = (1/2\sqrt{3})\mathrm{diag}(1,1,-2)$. The free energy in this phase is

$$\Omega_{mCFL} = -\frac{3\alpha_0^2}{16\beta}\left\{\left(\frac{T - T_c}{T_c} + \frac{4}{3}\eta\right)^2 + \frac{8}{3}\sigma^2\right\}. \tag{74}$$

As T increases, the first unlocking transition, the unlocking of Δ_2 (the pairing between Bu and Rs quarks), takes place at the critical temperature,

$$T_c^{\rm I} = \left(1 - \frac{16}{3}\sigma\right) T_c. \tag{75}$$

(ii) For $T_c^{\rm I} < T < T_c^{\rm II}$, $\Delta_2 = 0$ and

$$\Delta_i^2 = \frac{\alpha_0}{6\beta}\left(\frac{T_c - T}{T_c} + c_i\sigma\right), \tag{76}$$

with $c_{1,3} = (-7/3, 2/3)$. In this phase, we have only ud and ds pairings (the dSC phase), and there is a manifest symmetry, $U(1)_{C+L+R} \times U(1)_{C+L+R} \times U(1)_{C+V+B} \times U(1)_{C+V+B}$, where the corresponding $U(1)$ generators are

$$\begin{aligned}
\mathcal{Q}_1 &= T_3 - S_3, \\
\mathcal{Q}_2 &= T_8 - S_8, \\
\mathcal{Q}_3 &= Q + \frac{2}{\sqrt{3}} T_8 - 2S_3, \\
\mathcal{Q}_4 &= Q + \frac{2}{\sqrt{3}} S_8 - 2S_3,
\end{aligned} \tag{77}$$

respectively. Here $Q = 2/3$ is the generator of baryon charge (Q) and acts on the gap as Eq. (14). The free energy in this phase is

$$\Omega_{dSC} = -\frac{\alpha_0^2}{6\beta} \left\{ \left(\frac{T - T_c}{T_c} + \frac{5}{6}\eta \right)^2 + \frac{3}{4}\sigma^2 \right\}. \tag{78}$$

At $T = T_c^{\mathrm{II}}$, the second unlocking transition, the unlocking of Δ_1 (the pairing between Gs and Bd quarks), takes place at the critical temperature,

$$T_c^{\mathrm{II}} = \left(1 - \frac{7}{3}\sigma \right) T_c. \tag{79}$$

(iii) For $T_c^{\mathrm{II}} < T < T_c^{\mathrm{III}}$, one finds the 2SC phase, which has only ud pairing with

$$\Delta_3^2 = \frac{\alpha_0}{4\beta} \left(\frac{T_c - T}{T_c} - \frac{1}{3}\sigma \right). \tag{80}$$

The 2SC phase has a symmetry $SU(2)_C \times SU(2)_{L+R} \times U(1)_{C+B} \times U(1)_{L+R+B}$, where the corresponding $U(1)$ generators are

$$\begin{aligned}
\mathcal{Q}_5 &= Q + \sqrt{3} T_8, \\
\mathcal{Q}_6 &= Q + \sqrt{3} S_8,
\end{aligned} \tag{81}$$

respectively. The free energy in this phase is

$$\Omega_{2SC} = -\frac{\alpha_0^2}{8\beta} \left(\frac{T - T_c}{T_c} + \frac{1}{3}\sigma \right)^2. \tag{82}$$

The final unlocking transition where Δ_3 (the pairing between Rd and Gu quarks) vanishes occurs at

$$T_c^{\mathrm{III}} = \left(1 - \frac{1}{3}\sigma \right) T_c. \tag{83}$$

Above T_c^{III}, the system is in the normal phase. Note that in the temperature region $(T_c^{\mathrm{I}} - T)/T_c^{\mathrm{I}} < \mathrm{const} \cdot \sigma$, the gaps satisfy the condition (11), so the GL potential expanded up to quartic order in the gap is valid.

So far, we have derived the parameters $\beta_{1,2}$, ϵ, and η in the weak coupling approximation and discussed the phase structure expected at asymptotically high density. Now we relax the weak coupling constraint and study possible phase structures expected from the GL potential of the form Eq. (70) with arbitrary coupling strengths. To simplify the argument, we assume $\beta_1 = \beta_2 > 0$ and draw the phase diagram in the space of the parameters ϵ and η in Fig. 5.

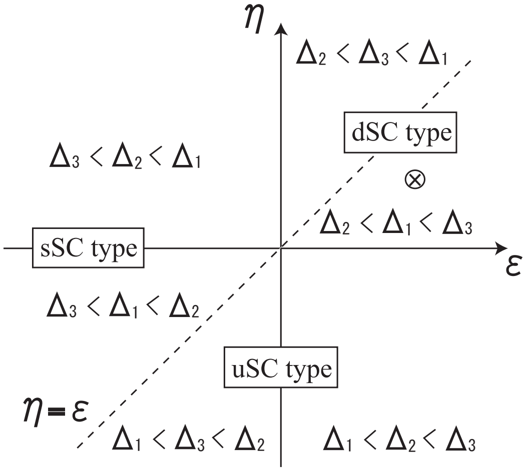

FIG. 5: The phase structure obtained from Eq. (70) in (ϵ, η) plane for $\beta_1 = \beta_2 > 0$. The mCFL phase is assumed to appear at sufficiently low temperature. ⊗ indicates the point calculated in the weak coupling approximation.

If we consider the case where the mCFL phase appears at temperature sufficiently below T_c, the relative magnitudes of the gaps behave as shown in Fig. 5. If Δ_2 is the smallest of the three gaps, we call the melting pattern "dSC-type" because the dSC phase would appear as T increases. "uSC-type" and "sSC-type" are defined in a similar way. As in Fig. 5, depending on the relative magnitude of ϵ and η, the dSC-type melting pattern is divided into two different classes in which the 2SC-type phase ($\Delta_1 \neq 0, \Delta_{2,3} = 0$ or $\Delta_3 \neq 0, \Delta_{1,2} = 0$) appears just below the transition temperature to the normal phase. The uSC-type and sSC-type melting patterns also have such a two-fold structure. The *hierarchical thermal unlocking* (mCFL → dSC → 2SC → normal) is realized in weak coupling as shown by ⊗ in the figure. The figure indicates that it is a rather robust phenomenon near the super-normal phase boundary. In other words, the uSC or sSC phase appears only when ϵ or η changes sign at least under the form of the GL potential in Eq. (70) with an assumption $\beta_1 = \beta_2 > 0$. We mention here that a recent analysis in Ref. [23] using the Nambu-Jona-Lasinio (NJL) model shows that the signs and the ratios of the coupling strengths in the GL potential take similar values with our weak coupling values: $\beta_1/\beta_2 = 1$ (with $\beta_1 > 0$ and $\beta_2 > 0$) and $\zeta \equiv \epsilon/\eta \cong 2$–$4$ (with $\epsilon > 0$ and $\eta > 0$).

B. Properties of quark and gluon modes

Next we resume considering about the weak coupling limit and discuss the properties of quark and gluon modes such as the excitation energies in each of the mCFL, dSC, and 2SC phases. The low energy excitations of these phases are massive or massless gauge bosons, gapped or gapless quark quasiparticles, and modes that are associated with fluctuations in the diquark fields. Here we concentrate on the gauge bosons and gapless fermions. As for gauge bosons, we only consider the transverse components of the gauge fields which, in the static limit, can become massive only in a superconductor. The longitudinal components are Debye screened in the vicinity of the transition temperature. Note that the "gapless fermions" in our previous paper [11] have been defined only by diagonalizing the self-energy Σ in Eq. (32). In the present paper, we have diagonalized the full propagator $G^{-1}(k)$ to define the gapless fermions in a more precise manner as will be shown below.

In Table I, we summarize the symmetries, the number of massive gauge bosons, and the number of gapless fermion modes in each phase. As we will show in detail below, the number of gapless quark modes depends not only on which phase we consider but also on the temperature itself. In each phase, in addition to the unpaired quark modes whose excitation energies are naturally zero, gapless modes appear if the temperature is in the region where the gaps satisfy the conditions listed in Table I.

In each phase, the gauge symmetry is broken partially or even totally. The Meissner masses for the general condensate, Eq. (69), and the corresponding massive (or massless) gauge fields can be calculated using the GL theory coupled to gluon fields [12] as

$$\begin{aligned}
&m_{A_1}^2 = m_{A_2}^2 = \kappa_T g^2(\Delta_1^2+\Delta_2^2),\\
&m_{A_4}^2 = m_{A_5}^2 = \kappa_T g^2(\Delta_1^2+\Delta_3^2),\\
&m_{A_6}^2 = m_{A_7}^2 = \kappa_T g^2(\Delta_2^2+\Delta_3^2),\\
&m_{A_8}^2 = \frac{4}{3}\kappa_T g^2\left(\frac{\Delta_1^2\Delta_2^2+\Delta_2^2\Delta_3^2+\Delta_3^2\Delta_1^2}{\Delta_1^2+\Delta_2^2}\right),\\
&m_{\tilde{A}}^2 = \frac{4}{3}\kappa_T g^2\left(\frac{\Delta_1^4+\Delta_2^4+\Delta_1^2\Delta_2^2}{\Delta_1^2+\Delta_2^2}\right).
\end{aligned} \tag{84}$$

Here $\tilde{A}$ is a mixed field of A_3 and A_8,

$$\begin{aligned}
\tilde{A} \;=\; &\frac{\sqrt{3}}{2}\frac{\Delta_1^2+\Delta_2^2}{\sqrt{\Delta_1^4+\Delta_2^4+\Delta_1^2\Delta_2^2}}A_3\\
&+\frac{1}{2}\frac{\Delta_1^2-\Delta_2^2}{\sqrt{\Delta_1^4+\Delta_2^4+\Delta_1^2\Delta_2^2}}A_8.
\end{aligned} \tag{85}$$

Here we followed the notations in Refs. [6, 12]. κ_T is the stiffness parameter which controls the spatial variation of the gap. In weak coupling it is proportional to the quartic coupling β as [12]

$$\kappa_T = \beta/3 = \frac{7\zeta(3)}{24(\pi T_c)^2}N(\mu). \tag{86}$$

We can reproduce the results in Table I in Ref. [24] by taking a limit $\Delta_{1,2}\to 0$ for the isoscalar 2SC phase and $\Delta_1=\Delta_2=\Delta_3$ for the CFL phase.

As given in a full description in Ref. [25], we can count the gapless quark modes by examining the spectra of which the full propagator diverges:

$$\det G^{-1}(E,\mathbf{q}) = \mathcal{G}_{Rd,Gu}\mathcal{G}_{Rs,Bu}\mathcal{G}_{Gs,Bd}\mathcal{G}_{Ru,Gd,Bs} = 0. \tag{87}$$

The gap matrix $\Sigma(k)$ can be written in block-diagonal form if we adequately take the base whereas the noninteracting quark propagator $G_0(k)$ is diagonal. The determinant Eq. (87) can be decomposed into three 4×4 determinants $\mathcal{G}_{Rd,Gu}$, $\mathcal{G}_{Rs,Bu}$, and $\mathcal{G}_{Gs,Bd}$, and one 6×6 determinant $\mathcal{G}_{Ru,Gd,Bs}$, which may effectively be written as

$$\begin{aligned}
\mathcal{G}_{Rd,Gu} \;=\; &\det\begin{pmatrix} \not q-\hat{p}_F^d & -\Delta_3\\ -\tilde{\Delta}_3 & \not q+\hat{p}_F^u\end{pmatrix}\\
\times\; &\det\begin{pmatrix} \not q-\hat{p}_F^u & -\Delta_3\\ -\tilde{\Delta}_3 & \not q+\hat{p}_F^d\end{pmatrix},
\end{aligned} \tag{88}$$

$$\begin{aligned}
\mathcal{G}_{Rs,Bu} \;=\; &\det\begin{pmatrix} \not q-\hat{p}_F^s & -\Delta_2\\ -\tilde{\Delta}_2 & \not q+\hat{p}_F^u\end{pmatrix}\\
\times\; &\det\begin{pmatrix} \not q-\hat{p}_F^u & -\Delta_2\\ -\tilde{\Delta}_2 & \not q+\hat{p}_F^s\end{pmatrix},
\end{aligned} \tag{89}$$

$$\begin{aligned}
\mathcal{G}_{Gs,Bd} \;=\; &\det\begin{pmatrix} \not q-\hat{p}_F^s & -\Delta_1\\ -\tilde{\Delta}_1 & \not q+\hat{p}_F^d\end{pmatrix}\\
\times\; &\det\begin{pmatrix} \not q-\hat{p}_F^d & -\Delta_1\\ -\tilde{\Delta}_1 & \not q+\hat{p}_F^s\end{pmatrix},
\end{aligned} \tag{90}$$

$$\begin{aligned}
&\mathcal{G}_{Ru,Gd,Bs} =\\
&\det\begin{pmatrix}
\not q-\hat{p}_F^u & 0 & 0 & 0 & \Delta_3 & \Delta_2\\
0 & \not q-\hat{p}_F^d & 0 & \Delta_3 & 0 & \Delta_1\\
0 & 0 & \not q-\hat{p}_F^s & \Delta_2 & \Delta_1 & 0\\
0 & \tilde{\Delta}_3 & \tilde{\Delta}_2 & \not q+\hat{p}_F^u & 0 & 0\\
\tilde{\Delta}_3 & 0 & \tilde{\Delta}_1 & 0 & \not q+\hat{p}_F^d & 0\\
\tilde{\Delta}_2 & \tilde{\Delta}_1 & 0 & 0 & 0 & \not q+\hat{p}_F^s
\end{pmatrix}.
\end{aligned} \tag{91}$$

Here $\hat{p}_F^i = p_F^i\gamma_0$, and p_F^i are the Fermi momenta of i quarks. Only in Eqs. (88)–(91) we abbreviate the Lorentz structure of the gap for simplicity; here Δ_i indicates $\gamma_5\Lambda^+\Delta_i$, and $\tilde{\Delta}_i$ indicates $\gamma_0(\gamma_5\Lambda^+\Delta_i)\gamma_0$. Moreover, we include the effect of m_s as a shift of the effective chemical potential p_F^i following Ref. [25]. Using Eqs. (40), (62), and (63), p_F^i's can be expressed as

$$\begin{aligned}
p_F^u &= \mu-(2/3)\mu_e,\\
p_F^d &= \mu+(1/3)\mu_e,\\
p_F^s &= \mu-(5/3)\mu_e.
\end{aligned} \tag{92}$$

In the vicinity of the critical temperature, chemical potential differences between colors $\delta\mu_{ab}$ can be ignored as stated in the previous sections.

As for the three 4×4 determinants, we can count the gapless modes as follows. First of all, (Rs,Bu) and

(Bu,Bd,Rs,Gs) quarks are gapless in the dSC and 2SC phases, respectively, because they do not participate in the pairing. Even for quarks participating in the pairing, they can produce gapless excitations near the critical point. As an example, consider a Fermi system composed of two species having different Fermi momenta, $p_F^{(1)}$ and $p_F^{(2)}$, and a superconducting gap Δ of pairing with each other. Then the quasiparticle spectra obtained after the diagonalization of the matrix fermion propagator can be gapless when the gap is smaller than half of the difference of the Fermi momenta,

$$|p_F^{(1)} - p_F^{(2)}| > 2\Delta. \tag{93}$$

In Ref. [26] the detailed analysis of the gapless superconductivity at finite temperature has been done; the chemical potentials and gaps have been calculated self-consistently at finite temperature.

In our case, the difference of the chemical potentials depends on temperature only in higher orders so that the left hand side of Eq. (93) can be regarded as constant in temperature. Then, we can solve Eq. (93) analytically using Eqs. (72), (76), and (80). When the conditions shown below for the mCFL, dSC and 2SC phases are satisfied, we obtain two more gapless modes in each phase. The conditions are

- for the mCFL phase, $\Delta_2 < \frac{1}{2}\mu_e$.
- for the dSC phase, $\Delta_1 < \mu_e$.
- for the 2SC phase, $\Delta_3 < \frac{1}{2}\mu_e$.

For example, let us consider the temperature satisfying $T_c^{\rm III} < T < T_c^{\rm II}$ (the dSC region). We basically have two unpaired quark modes (Bu and Rs). Additionally, if the temperature satisfies $\Delta_1 < \mu_e$, then we obtain two more gapless modes.

We move on to the 6×6 determinant. In this sector, there are basically no unpaired quark modes in the dSC and mCFL phases and one unpaired quark mode (Bs) in the 2SC phase. In order to find additional gapless modes, we examine the solutions which satisfy the equation

$$\begin{aligned} 0 &= \mathcal{G}_{Ru,Gd,Bs}(E=0,\mathbf{q})^{1/2} \\ &= (|\mathbf{q}|+p_F^u)^2(|\mathbf{q}|+p_F^d)^2(|\mathbf{q}|+p_F^s)^2 \\ &\quad [\{x(x-\mu_e)(x+\mu_e)+x\Delta_1^2+(x-\mu_e)\Delta_2^2 \\ &\qquad +(x+\mu_e)\Delta_3^2\}^2+4\Delta_1^2\Delta_2^2\Delta_3^2]. \end{aligned} \tag{94}$$

Here $x = |\mathbf{q}| - \bar{\mu}$, where $\bar{\mu} = \mu - 2\mu_e/3$ is the chemical potential averaged over Ru, Gd, and Bs quarks. Then we find

- for the mCFL phase, no more gapless modes.
- for the dSC phase, one more gapless mode corresponding to the mixture of Ru, Gd, and Bs quarks.
- for the 2SC phase, if the gap satisfies $\Delta_3 < \frac{1}{2}\mu_e$, we obtain two more gapless modes corresponding to the mixtures of Ru and Gd quarks.

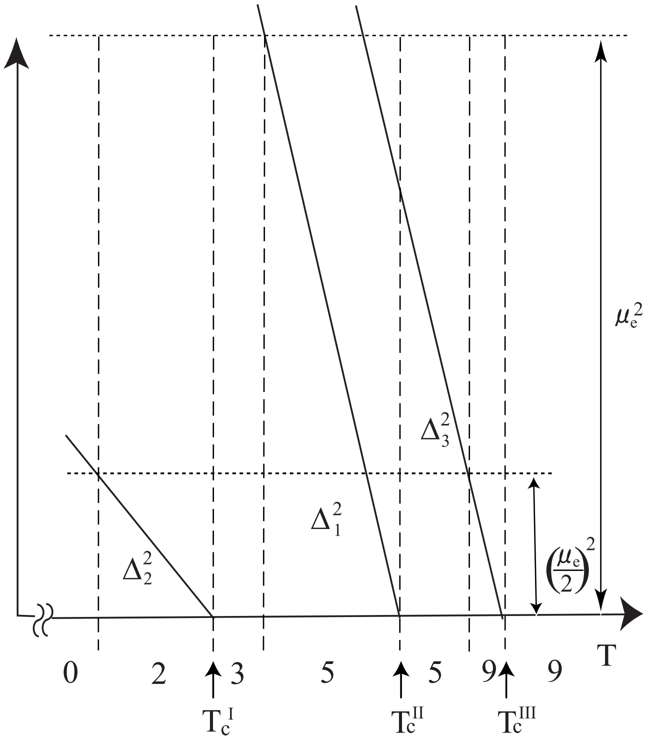

FIG. 6: The number of gapless quark modes as a function of temperature, together with the gaps and the electron chemical potential.

In Fig. 6, we show the number of gapless quark modes together with the gaps as a function of temperature. We can see that the gapless modes always exist just below the critical temperatures $T_c^{\rm I}$, $T_c^{\rm II}$, and $T_c^{\rm III}$. The number of the gapless modes decreases as the temperature lowers at high density.

VI. SUMMARY AND CONCLUDING REMARKS

In this paper, we have investigated thermal phase transitions of the color superconducting quark matter in the presence of finite strange quark mass and under charge neutrality. We constructed a general form of the GL potential in such a way that it fulfills symmetry constraints and then obtained the weak coupling expression for the GL potential including the corrections from unequal quark masses (m_i, i=u,d,s) and unequal quark chemical potentials (μ_i, i=u,d,s). The corrections to the quadratic term of the GL potential from m_i and μ_i indicate that it is the *average* density of states of paired quarks which determines the critical temperatures of different pairs, as can be seen in Eqs. (57) and (58).

We found that the effects of the strange quark mass (m_s) through the mass term in the quark propagator and through the electron charge chemical potential play a vital role near the super-normal phase boundary, while the color neutrality plays a minor role in contrast to the case at zero temperature.

As shown in Figs. 3 and 4, an interplay between these two effects of m_s splits the single phase transition (CFL → normal) for the *u*-*d*-*s* symmetric system to three successive second-order phase transitions (mCFL → dSC → 2SC → normal). The window of the "dSC" phase opened up between the 2SC and mCFL phases is a new phase where only the superconducting gaps with *d* quarks are non-vanishing [11].

The obtained phase structure, which is shown to be valid in the weak coupling (high density) region, may be applicable even in the strong coupling region as long as the successive transitions driven by the quadratic term of the GL potential take place in a small interval of temperature near the super-normal phase boundary. In connection with this, it was shown recently that the dSC phase discussed in the present paper may be replaced by the uSC phase in the low density region through a "doubly critical" point on the basis of the NJL model [23] (see also Ref. [27]). Moreover, if we take into account the chiral condensate at low density, some interplay between the broken chiral symmetry and the color superconductivity is expected [28]. How to incorporate these aspects in our picture based on the GL potential is an interesting open problem.

In the present paper, the properties of quark and gluon modes such as the excitation energies were also investigated. The excitation spectra of quarks indicate that in addition to unpaired quark modes, whose excitation energy is naturally zero, more than one gapless mode appear just below each critical temperature as summarized in Table I. Effects of the gapless modes on physical phenomena such as neutron star cooling is an interesting problem to be examined [29].

Throughout this paper, we have studied the phase transitions in the mean-field level. In weak coupling, thermal fluctuations of the gluon fields could change the second-order transition to the first-order one as described in Refs. [24, 30]. As far as the order of phase transition is concerned, the gluon fluctuations have the following effects (the detailed account will be given in our future publication): The second order transition, mCFL → dSC, remains second order. This is because all eight gluons are Meissner screened across $T = T_c^{\mathrm{I}}$ and thus cannot induce a cubic term in the order parameter in the GL potential. On the other hand, the transitions, dSC → 2SC and 2SC → normal, become weak first order since some of the gluons become massless at $T = T_c^{\mathrm{I,II}}$ (Table I). In order to obtain a final phase diagram we should study the competition between the shift of the critical temperature discussed in the present paper and that coming from the fluctuation effects.

Acknowledgments

We are grateful to H. Abuki, G. Baym, K. Fukushima, and M. Huang for helpful discussions. K.I., M.T., and T.H. thank the Institute for Nuclear Theory, Univ. of Washington where a part of this work has been completed. They also thank K. Rajagopal, I. Shovkovy, T. Schäfer, and C. Kouvaris for discussions. This work was supported in part by RIKEN Special Postdoctoral Researchers Grant No. A12-52010, and by the Grants-in-Aid of the Japanese Ministry of Education, Culture, Sports, Science, and Technology (No. 15540254).

[1] D. Bailin and A. Love, Phys. Rep. **107**, 325 (1984); M. Iwasaki and T. Iwado, Phys. Lett. B **350**, 163 (1995); M. Alford, K. Rajagopal, and F. Wilczek, Phys. Lett. B **422**, 247 (1998); R. Rapp, T. Schäfer, E.V. Shuryak, and M. Velkovsky, Phys. Rev. Lett. **81**, 53 (1998).

[2] For reviews, see K. Rajagopal and F. Wilczek, in *Handbook of QCD*, edited by M. Shifman (World Scientific, Singapore, 2001); M.G. Alford, Ann. Rev. Nucl. Part. Sci. **51**, 131 (2001).

[3] D. T. Son, Phys. Rev. D **59**, 094019 (1999).

[4] T. Schäfer, Nucl. Phys. **B575**, 269 (2000).

[5] N.J. Evans, J. Hormuzdiar, S.D.H. Hsu, and M. Schwetz, Nucl. Phys. **B581**, 391 (2000).

[6] K. Iida and G. Baym, Phys. Rev. D **63**, 074018 (2001); *ibid.* **66**, 059903(E) (2002).

[7] D.K. Hong and S.D.H. Hsu, Phys. Rev. D **68**, 034011 (2003).

[8] M. Alford, K. Rajagopal, and F. Wilczek, Nucl. Phys. **B537**, 443 (1999).

[9] A. Schmitt, Q. Wang, and D.H. Rischke, Phys. Rev. D **66**, 114010 (2002).

[10] M. Alford, J. Berges and K. Rajagopal, Phys. Rev. Lett. **84**, 598 (2000); M. Huang and I. Shovkovy, Nucl. Phys. **A729**, 835 (2003); M. Alford, C. Kouvaris, and K. Rajagopal, Phys. Rev. Lett. **92**, 222001 (2004).

[11] K. Iida, T. Matsuura, M. Tachibana, and T. Hatsuda, Phys. Rev. Lett. **93**, 132001 (2004).

[12] K. Iida and G. Baym, Phys. Rev. D **66**, 014015 (2002).

[13] J.M. Luttinger and J.C. Ward, Phys. Rev. **118**, 1417 (1960); G. Baym, Phys. Rev. **127**, 1391 (1962); J.M. Cornwall, R. Jackiw, and E. Tomboulis, Phys. Rev. D **10**, 2428 (1974).

[14] H. Georgi, *Weak Interactions and Modern Particle Theory*, (W.A. Benjamin, Menlo Park, CA, 1984).

[15] R.D. Pisarski and D.H. Rischke, Phys. Rev. D **60**, 094013, (1999).

[16] D.K. Hong, Nucl. Phys. **B582**, 451 (2000); W.E. Brown, J.T. Liu, and H.C. Ren, Phys. Rev. D **62**, 054016 (2000).

[17] R.D. Pisarski and D.H. Rischke, Phys. Rev. D **61**, 074017 (2000).

[18] R.D. Pisarski, Phys. Rev. C **62**, 035202 (2000).

[19] M.G. Alford, J. Berges, and K. Rajagopal, Nucl. Phys.

TABLE I: The symmetry, the number of Meissner screened gluons, and the number of gapless fermion modes in the mCFL, dSC, and 2SC phases. The results for the Meissner masses are given in Eq. (84). In each phase, if the temperature is in the region where the gaps satisfy the conditions listed in this table, more gapless modes appear in addition to unpaired quark modes. $(\cdots)$ shows the color and flavor of unpaired quarks. $\{\cdots\}$ shows which combination of quarks makes the gapless modes.

	Symmetry	Number of massive gluons	Number of gapless quark modes				
			unpaired quarks	paired quarks			
				$\Delta_3 < \mu_e/2$	$\Delta_1 < \mu_e$	$\Delta_2 < \mu_e/2$	no condition
mCFL	$[U(1)]^2$	8	0	-	-	2 $\{Rs, Bu\}$	-
dSC	$[U(1)]^4$	8	2 (Rs, Bu)	-	2$\{Gs, Bd\}$	-	1$\{Ru, Gd, Bs\}$
2SC	$[SU(2)]^2 \times [U(1)]^2$	5	5 (Bu, Bd, Bs, Rs, Gs)	2 $\{Rd, Gu\}$ 2 $\{Ru, Gd\}$	-	-	-

B558, 219 (1999); T. Schäfer and F. Wilczek, Phys. Rev. D **60**, 074014 (1999).

[20] H. Abuki, Prog. Theor. Phys. **110**, 937 (2003).

[21] D.D. Dietrich and D.H. Rischke, Prog. Part. Nucl. Phys. **53**, 305 (2004).

[22] T. Schäfer, Phys. Rev. D **65**, 094033 (2002).

[23] K. Fukushima, C. Kouvaris, and K. Rajagopal, hep-ph/0408322.

[24] T. Matsuura, K. Iida, T. Hatsuda, and G. Baym, Phys. Rev. D **69**, 074012 (2004).

[25] M. Alford, C. Kouvaris, and K. Rajagopal, Phys. Rev. Lett. **92**, 222001 (2004); M. Alford, C. Kouvaris, and K. Rajagopal, hep-ph/0406137.

[26] I. Shovkovy and M. Huang, Phys. Lett. B **564**, 205 (2003); M. Huang, and I. Shovkovy, Nucl. Phys. **A729**, 835 (2003).

[27] S.B. Ruster, I.A. Shovkovy, and D.H. Rischke, Nucl. Phys. **A743**, 127 (2004).

[28] See, e.g., M. Buballa, hep-ph/0402234 and references therein.

[29] T. Schäfer and K. Schwenzer, astro-ph/0410395; M. Alford, P. Jotwani, C. Kouvaris, J. Kundu, and K. Rajagopal astro-ph/0411560.

[30] I. Giannakis, D.f. Hou, H.c. Ren, and D.H. Rischke, hep-ph/0406031.